Available online at www.sciencedirect.com
SCIENCE DIRECT
Journal of the European Ceramic Society 26 (2006) 317–321
www.elsevier.com/locate/jeurceramsoc

Spectroscopic study of a Ni-bearing gahnite pigment

Giada Lorenzi[a], Giovanni Baldi[a], Francesco Di Benedetto[b,*], Valentina Faso[a], Pierfranco Lattanzi[c], Maurizio Romanelli[d]

[a] *Laboratorio di Ricerca Avanzata, Colorobbia Group, via Pietramarina 123, I50053 Sovigliana, Vinci, Italy*
[b] *Museo di Storia Naturale, Università di Firenze, Via G. La Pira 4, I50121 Firenze, Italy*
[c] *Dipartimento di Scienze della Terra, Università di Cagliari, Via Trentino, 51, I09127 Cagliari, Italy*
[d] *Dipartimento di Chimica, Università di Firenze, via della Lastruccia 3, I50019 Sesto, Fiorentino, Italy*

Received 25 June 2004; received in revised form 13 October 2004; accepted 24 October 2004
Available online 7 January 2005

Abstract

In the course of the synthesis of a blue Ni-bearing gahnite ($ZnAl_2O_4$), a green phase was often observed contaminating the blue products of the synthesis, thus affecting the chromatic stability of the material. Both the blue and the green phases were characterised by means of X-ray powder diffraction (XRD) and diffuse reflectance spectroscopy (DRS), in order to understand the nature of the blue colour and of the contamination.

For both phases, the Rietveld refinement of the XRD powder patterns indicates that gahnite is indeed the main phase present. The blue product also contains minimal amounts of corundum (Al_2O_3). The colour of the blue phase was related to the tetrahedral crystal field surrounding Ni^{2+} in gahnite. Nevertheless, only a small fraction of tetrahedrally coordinated Ni was determined, being this ion mostly distributed over the octahedral sites. The green phase is apparently homogeneous, both under the electron microscope and from interpretation of XRD. However, from the DRS spectrum, it is suggested that the green colour could result from a mixture of the blue Ni-bearing gahnite and a small fraction of yellow–green NiO. Probably because of its low amount and/or poor crystallinity, this latter phase is undetectable by XRD. The nature of the chromatic instability of the final products of the synthesis is, therefore, ascribed to an incomplete Ni incorporation in the spinel structure.

Keywords: Optical properties; Rietveld refinement; Spectroscopy; Spinels; Transition metal oxides; Pigments

1. Introduction

Spinel-type oxides ($Me^{2+}Me_2{}^{3+}O_4$) represent one of the most studied class of materials in solid-state science, because of their relevant magnetic, refractory, semiconducting, and colouring properties. They are stable even under drastic thermal and redox industrial treatments. The incorporation of transition metal (TM) ions into stable diamagnetic spinels is a successful process to obtain materials with peculiar physical properties and, sometimes, a very intense colour. The colouring properties of the spinels obtained by this approach are mainly determined by the crystal field surrounding the TM ion, i.e. by its d–d and/or charge transfer transitions. A large number of cations can be accommodated in the spinel structure.[1] Moreover, these cations can occupy two sites, T, tetrahedral, and O, octahedral, respectively. All distribution ratios are allowed in spinels, from the *normal* type (Me^{3+} in the O sites) to the *inverse* type (Me^{2+} in one half of the O sites), as a function of chemical composition and temperature. The possible presence of several TM cations in different coordination accounts for the variety of colours that can be obtained.

Natural and synthetic blue pigments are widely used in the ceramic industry as colouring agents in glazes and coloured stoneware. The traditional and currently most used source of blue is represented by the cobalt ion.[2] However, the synthesis of Co-based blue pigments presents problems concern-

* Corresponding author. Fax: +39 055 284571.
E-mail address: dibenefr@geo.unifi.it (F. Di Benedetto).

0955-2219/$ – see front matter © 2004 Elsevier Ltd. All rights reserved.
doi:10.1016/j.jeurceramsoc.2004.10.027

ing the production costs and the environmental impact of the manufacturing process. Hence, there is much effort for developing new blue pigments,[3,4] by doping with efficient chromophores white or colourless stable structures, such as gahnite ($ZnAl_2O_4$). A specific research study, performed by the Advanced Materials Laboratory of the Colorobbia Group, developed a blue Ni-bearing gahnite, potentially interesting for industrial applications. This material incorporates fairly low amounts of Ni, thus reducing both the environmental problems related to the well-documented Ni toxicity, and the potential production costs. However, the yield of the synthetic reaction at the laboratory scale was found to be largely dependent on experimental conditions, i.e. the ramp speed, the temperature and length of the thermal treatment, and the role of the mineralising agents. In particular, in several runs a green phase was found to contaminate the final products, affecting the chromatic stability of the material.

A study of the origin of the blue colour of the Ni-bearing pigment has been undertaken, in order to understand the nature of the contamination. The two phases, blue and green, were separated and characterised by X-ray powder diffraction (XRPD), and by diffuse reflectance spectroscopy (DRS) in the UV–vis region.

2. Experimental procedures

Ni-bearing gahnite was prepared by mixing commercial reagents. A mixture of ZnO, Al_2O_3 and $NiCO_3$ (48.0, 49.5 and 2.5 mol%, respectively) was homogenised, dry milled, to improve the powder reactivity during the thermal treatment, and heated in a high temperature furnace (Lenton EHF 1700) in alumina crucibles. The thermal treatment consisted in a temperature increase from room temperature up to 1400 °C in 6 h, and a plateau of 4 h at 1400 °C. Extremely fine, coloured powders were obtained after cooling in air and crumbling. The blue Ni-bearing pigment studied here corresponds to the synthesis run labelled as PG Ni3, whereas the green phase was manually isolated under the binocular microscope, from the powders of run PG Ni1. The two products will be hereafter labelled as Ni–B and Ni–G, respectively. Both phases were found homogeneous in particle shape, dimension and colour at the binocular microscopic observation. Back-scattered electron images, recorded at the scanning electron microscope, confirmed the apparent chemical homogeneity of both phases. Specifically, SEM-EDAX analyses indicated a chemical composition $Zn_{0.95}Ni_{0.05}Al_2O_4$ for both samples, in good agreement with molar proportions in the run charge.

High quality X-ray powder diffraction (XRD) patterns were obtained using a Philips PW 3710 diffractometer with Cu anode and graphite monochromator, equipped with PC-X'Pert Pro software for data acquisition and handling. Experimental conditions were: 20 mA, 40 kV, 10–140° 2θ, step size 0.02° 2θ, 2 s per step, plexiglas support. The powder structural refinement was carried out through the Rietveld algorithm using the Rietquan software.[5]

Spectroscopic investigations were performed by means of a Perkin Elmer Lambda 800 UV–vis spectrometer equipped with an integration sphere. The diffuse reflectance spectra were acquired from 300 to 800 nm with a step size of 1 nm. The spectra were automatically converted to absorbance spectra by using the Kubelka–Munk function.[6] Spectral profiles were fitted by means of Microcal Origin 6.0 package, assuming Gaussian line shapes.

3. Results

3.1. XRD

In Figs. 1 and 2 the XRD powder patterns of both samples are shown. The reaction products consist mainly of gahnite, $ZnAl_2O_4$. In addition, the Ni–B charge contains also a minor amount of corundum, Al_2O_3. As a consequence, Ni^{2+} has been assumed to be incorporated in gahnite, substituting for Zn^{2+}, in both Ni–B and Ni–G powders.

The Rietveld refinement has been performed, in order to determine both the quantitative phase composition of Ni–B and the site distribution of Ni in the two samples. The total amount of Ni in gahnite (0.05 afu) was not refined, and kept constant. Moreover, the presence of a very small amount of corundum (1.6 wt.% according to the refinement) in Ni–B was assumed to have a negligible influence on the overall gahnite chemical composition. The mean crystallite dimension of gahnite was found to be fairly small in both charges, ranging between 100 and 300 nm (Table 1). This was also confirmed by electron microscopy observations. The distribution of Ni between the T and O sites was refined, assuming Zn to be present only in the T site.[1] The obtained results are listed in Table 1. The powder pattern, relative to the cubic gahnite structure, appears rather insensitive to the Ni location: Ni and Zn have similar X-ray scattering factors, and the relatively large difference for Ni and Al does not induce significant pattern variations, because of the low amount of Ni

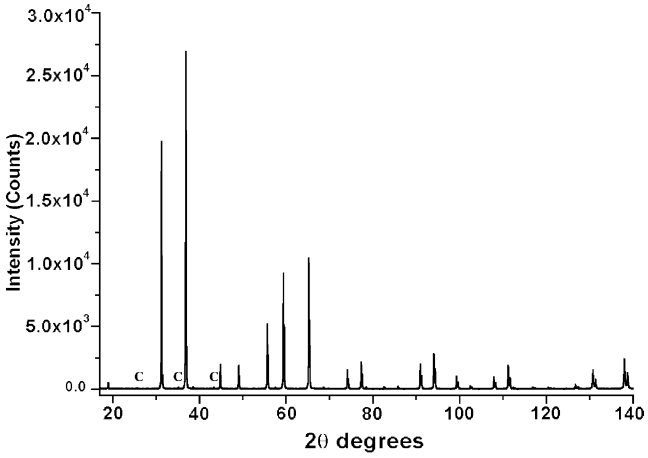

Fig. 1. XRPD pattern of sample Ni–B ("C" denotes the most intense corundum reflections).

Table 1
Rietveld refinements results: phase composition, oxygen parameter, lattice constants and crystallite dimension

Samples	Phase composition (wt.%)		x_O	a (Å)	Crystal dimension (nm)
Ni–B	98.4(4)	Gahnite	0.3891(1)	8.0850(1)	320
	1.6(1)	Corundum			
Ni–G	100	Gahnite	0.3889(1)	8.0873(1)	130

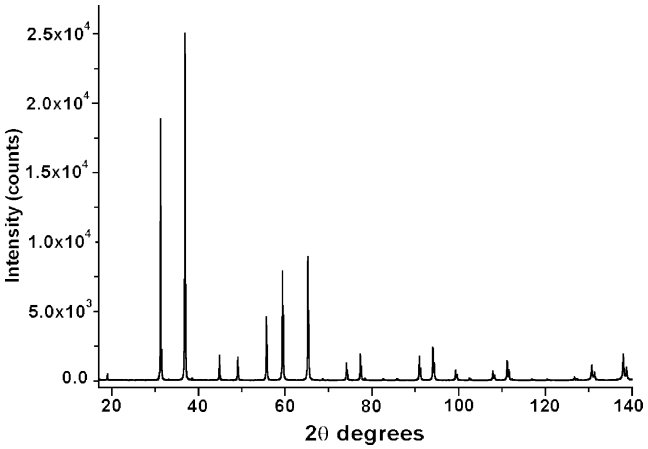

Fig. 2. XRPD pattern of sample Ni–G.

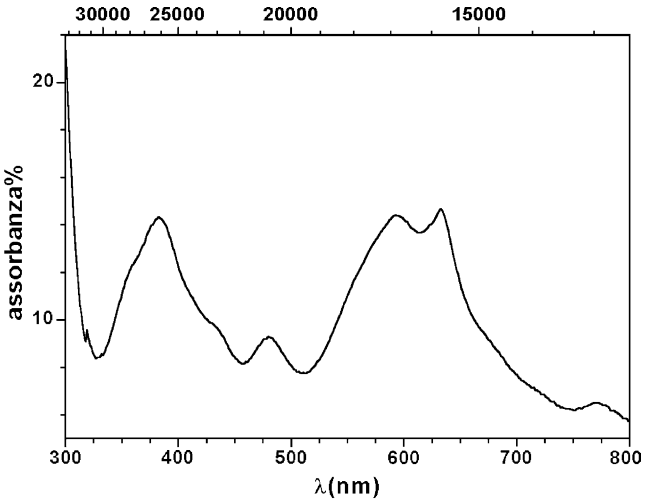

Fig. 3. Absorption vs. wavelength spectra of Ni–B.

(0.05 afu). The attempt to refine the Ni distribution between the T and O sites was unsuccessful. The numerical convergence of the least squares algorithm occurred by assigning most of the Ni to the O site, in agreement with the literature.[1] On the other hand, repeated refinements yielded very different distribution results, thus suggesting that the large uncertainty of the refinement does not allow to conclusively assign the Ni position.

3.2. DRS

The DRS spectra of Ni–B and Ni–G are presented, as absorbance (A%) versus wavelength (λ), in the range 300–800 nm, in Figs. 3 and 4, respectively. In Ni–B spectrum, four intense absorption bands, due to crystal field transitions, are observed at 630, 600, 480 and 380 nm, respectively. The 600 and 380 bands present a shoulder at lower wavelength values, 570 and 350 nm, respectively. Two further weak bands can be observed at 770 and 430 nm. The spectrum of Ni–G closely resembles the spectrum of Ni–B in the range 520–800 nm. At lower λ values, a broad band, centred at ∼380 nm, hides any other effect.

4. Discussion

On the basis of the XRD powder patterns, no significant differences have been detected between Ni–B and Ni–G, apparently suggesting gahnite to be the only phase hosting Ni. Even if all coordination numbers from 7 to 2 are observed for Ni^{2+},[7,8] this ion manifests a marked preference for octahedral coordination, occurring in tetrahedral configuration if forced by external constraints. As a consequence, Ni^{2+}, tending to occupy the O sites only, has been observed to induce a consistent inversion of the spinel structure.[1] However, few studies investigate the low content range behaviour (e.g. Ni in the spinel sensu strictu[9]). The distribution of Ni between the T and O sites may result affected also by its concentration, and by the nature of the other ions (Zn, Mg, ...) involved. Moreover, in synthetic spinel systems, the degree of inversion may vary as a function of the temperature of synthesis ($T > 1000\,^{\circ}C$) and of quenching/annealing[10], because of a T-dependent cation disorder.[11,12] In general, Ni^{2+} can be

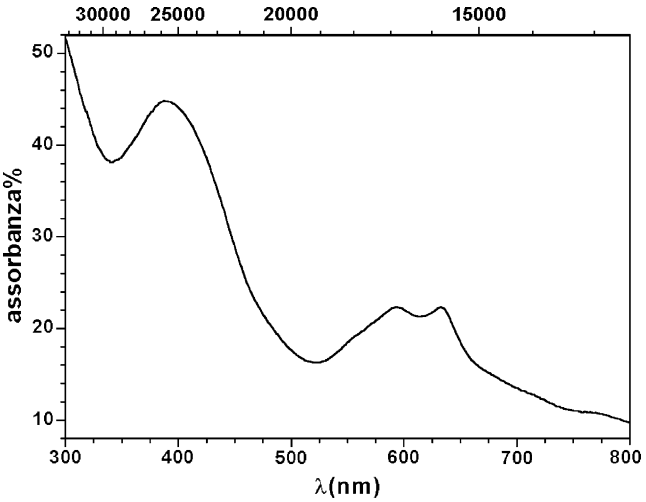

Fig. 4. Absorption vs. wavelength spectra of Ni–G.

Table 2
Optical transitions for tetrahedral (left) and octahedral (right) Ni^{2+}

Band	Transition	Band	Transition
$\nu 1_{Td}$	$^3T_1 \rightarrow {}^3T_2$ (^3F)	$\nu 1_{Oh}$	$^3A_{2g} \rightarrow {}^3T_{2g}$ (^3F)
$\nu 2_{Td}$	$^3T_1 \rightarrow {}^3A_2$ (^3F)	$\nu 2_{Oh}$	$^3A_{2g} \rightarrow {}^3T_{1g}$ (^3F)
($\nu 3_{Td}$)	$^3T_1 \rightarrow {}^1T_2$, ^1E (^1D)	($\nu 3_{Oh}$)	$^3A_{2g} \rightarrow {}^1E_g$ (^1D)
		($\nu 4_{Oh}$)	$^3A_{2g} \rightarrow {}^1T_{2g}$ (^1D)
$\nu 4_{Td}$	$^3T_1 \rightarrow {}^3T_2$ (^3P)	$\nu 5_{Oh}$	$^3A_{2g} \rightarrow {}^3T_{1g}$ (^3P)
($\nu 5_{Td}$)	$^3T_1 \rightarrow {}^1T_2$ (^1G)	($\nu 6_{Oh}$)	$^3A_{2g} \rightarrow {}^1A_{1g}$ (^1G)

assumed to always prefer the O site, even if the presence of a fraction in the T-site cannot be ruled out.[9,11–14]

According to the Tanabe–Sugano diagram of a d^8 ion in cubic coordination,[1,15] three spin-allowed d–d transitions can occur in both the tetrahedral and octahedral electronic spectra (see Table 2). In addition, spin-forbidden transitions to the singlet excited states can also be observed in the visible and near-ultraviolet regions.[8,16] The degenerate excited states of T and E symmetry may be resolved into additional energy levels, due either to a non-cubic local symmetry[1] or to spin–orbit interaction.[15] The values of the tetrahedral splitting 10 Dq reported in literature for Ni in oxo-coordination,[1,8,15] usually ~4500 cm^{-1}, imply that the two spin-allowed d–d transition $\nu 2_{Td}$ and $\nu 3_{Td}$ are of low energy, and fall in the NIR range, i.e. outside of the investigated range of energies of this study (12,500–33,300 cm^{-1}). The electronic transitions reported in literature for Ni^{2+} in several oxide structures with regular or distorted octahedral sites[1,16] present roughly similar octahedral splitting 10 Dq values of 8500–10,500 cm^{-1}. As a consequence, the $\nu 1_{Oh}$ transition, corresponding exactly to the 10 Dq separation, is always undetectable in the UV–vis range. The intensities of tetrahedral, non-centrosymmetric transitions are typically 10–100 higher than those observed for the same ion in a centrosymmetric ligand environment, such as in octahedral coordination.[15] Because some tetrahedral and octahedral bands may occur at similar energy values, the experimental intensity was taken into account, to establish the correct attribution.

The band attribution for the investigated samples (Table 3) suggests the simultaneous presence of tetrahedral and octahedral Ni^{2+}. Even if, in fact, the XRD data point out the prevailing fraction of Ni in O sites, the overall spectral shape of both samples in the region 12,500–22,000 cm^{-1} presents a clear fingerprint of tetrahedral Ni.[8] The main absorption band observed in Ni–B at ~15,820 cm^{-1} (632 nm) corresponds to the $\nu 4_{Td}$ transition. Moreover, the two bands at 12,950 and 20,790 cm^{-1} can be assigned to spin-forbidden $\nu 3_{Td}$ and $\nu 5_{Td}$ transitions, usually observed in solids.[8,15] Tetrahedral Ni, which substitutes for Zn into a site with cubic point symmetry, does not present tetragonal or trigonal distortion. Nevertheless, as pointed out by Weakliem,[15] the effect of the spin–orbit interaction induces a further very small splitting, which results in the presence of structured bands (Fig. 3). The $\nu 4_{Td}$ transition, in particular, is the convolution of four spin–orbit transition[15] and appears clearly split (peaks at 15,820 and

Table 3
Band position (in nm and cm^{-1}) and relative assignment for the investigated samples

Band position				Assignment
Ni–B		Ni–G		
nm	cm^{-1}	nm	cm^{-1}	
771	12,970	778	12,850	($\nu 3_{Td}$)
688	14,535	690	14,492	
634	15,773	632	15,820	$\nu 4_{Td}$
593	16,863	594	16,830	
479	20,876			($\nu 5_{Td}$)
430	23,256			CT
384	26,042			
351	28,490			$\nu 5_{Oh}$

The band labels are referred to Ni^{2+} in the O site (see text).

16,860 cm^{-1}). The further intense band at ~26,000 cm^{-1} may be ascribed to the lowest-energy charge-transfer (CT) transition, which has been reported to occur ranging between 35,000 cm^{-1}, in $ZnSiO_4$[8] and 22,500 cm^{-1}, in ZnO.[15]

The bands due to octahedral Ni cannot be easily detected in presence of tetrahedral Ni, due to the large difference in intensity.[15] Nevertheless, a tentative identification has been performed with reference to the Burns's[1] data for Ni_{Oh} in spinel, $MgAl_2O_4$. This author observed the two spin-allowed d–d transitions at 16,000 ($\nu 2_{Oh}$) and 27,000 cm^{-1} ($\nu 5_{Oh}$), respectively. The first region is fully hidden by the main $\nu 5_{Td}$ transition, whereas the second can be observed as a shoulder of the CT band.

The electronic spectrum of Ni–G in the range 12,500–19,000 cm^{-1} presents bands at 12,850, 14,492, 15,820 and 16,830 cm^{-1}, whose absolute intensities closely corresponds to those of Ni–B. The reproducibility of the spectral features, including intensities, suggests that a similar partitioning of Ni^{2+} between the T and O sites has been reached. On the other hand, the broad absorption at ~25,000 cm^{-1} appears definitely different, and cannot be related to d–d transition of tetrahedral/octahedral Ni^{2+}. Moreover, the onset of the lowest-energy CT band in Ni-bearing $MgAl_2O_4$ has been observed well above the experimental energy value found here, being the $\nu 5_{Oh}$ energy 27,000 cm^{-1}. The possible attribution of this band to octahedral Ni in the gahnite host appears definitely feeble. On the contrary, the presence of a broad band at ~25,000 cm^{-1}, and of a charge transfer absorption edge starting at 25,000–28,000 cm^{-1}, is characteristic of octahedral Ni^{2+} in NiO.[16,17] This electronic transition was also found to depend on the crystallinity of the nickel oxide, so that the green crystallised product becomes yellow if nanocrystalline, because of the increased intensity of the ramp at 350–400 nm.[17]

On the basis of these considerations, the attribution of the ~20,800 cm^{-1} spectral band of Ni–G to a small fraction of NiO has been, therefore, preferred. The absence of reflections relative to this phase in the XRD powder pattern can be explained either by its very low amount and/or by its poor crystallinity. A refinement of the experimental Ni–G XRD

powder pattern was attempted including NiO (bunsenite) in the assemblage: the best fit results indicated 0.25 wt.% NiO as the minimum detection limit in the experimental conditions of the pattern. This value, in the assumption of crystalline bunsenite, gives an upper estimate of the amount of NiO occurring in this sample as a separate phase. On the other hand, higher amounts of poorly or non-crystalline NiO might go undetected. The characteristic charge transfer transitions of NiO present high values of molar absorptivity.[17] Hence, a highly colouring effect of this species is conceivable even in very low amounts. As previously reported, Ni–G appears homogeneous at the optical and electron microscopic observations. This suggests a uniform distribution of NiO within the charge. An alternative explanation is that it forms thin rims around the blue phase.

5. Conclusions

Consideration of all experimental results leads to the conclusion that the blue product Ni–B is mainly Ni-bearing gahnite (with a small amount of corundum), whereas green Ni–G appears a mixture of Ni-bearing gahnite and small amounts of NiO. The formation of NiO is ascribed to decomposition of the reactant used, $NiCO_3$, and incomplete reaction to form Ni-bearing gahnite. The presence of the nickel oxide as a contaminant represents a relevant difficulty for industrial applications: the intimate association of blue Ni-gahnite and unreacted NiO modifies not only the chromatic stability of the pigment, but also the final colour of the glaze, because the contaminant oxide may react with the glass to form coloured products.[18]

In spite of this limitation, Ni-bearing gahnite proved to represent a very interesting pigment, where the fundamental role of tetrahedral Ni^{2+} to determine the colouring properties of the material has been established. The fraction of tetrahedral Ni^{2+}, in fact, has been found rather small, but strongly related to the colour of the pigment. The low Ni-content, the high temperature treatment and the preference of Zn for the T-site favour the incorporation of most of Ni in the O site, but the electronic transitions of this latter species are of low intensity, and do not substantially affect the pigment colour. On the basis of the present data, no evidence of significant variations of the ratio Ni_{Td}/Ni_{Oh} were observed. This consideration is in agreement with a temperature-dependent cation disorder mechanism as source of tetrahedral Ni. As a consequence, the blue Ni-gahnite pigment is characterised by a stability, which may warrant its utilisation to realise blue pigments for the ceramic industry.

Acknowledgements

The authors are indebted to G.P. Bernardini for critical reading of this manuscript. A. Dei is sincerely thanked for useful discussion of the diffuse reflectance data. The manuscript greatly benefited from the careful revision by an anonymous referee.

References

1. Burns, G. R., *Mineralogical Applications of Crystal Field Theory*. University Press, Cambridge, 1993.
2. Melo, D. M. A., Cunha, J. D., Fernandes, J. D. G., Bernardi, M. I., Melo, M. A. F. and Martinelli, A. E., *Mater. Res. Bull.*, 2003, **38**, 1559–1564.
3. Llusar, M., Fores, A., Badenes, J. A., Calbo, J., Tena, M. A. and Monros, G., *J. Eur. Ceram. Soc.*, 2001, **21**, 1121–1130.
4. Andreozzi, G. B., Baldi, G., Bernardini, G. P., Di Benedetto, F. and Romanelli, M., *Eur. J. Ceram. Soc.*, 2004, **24**, 821–824.
5. Lutterotti, L., Ceccato, R., Dal Maschio, R. and Pagani, E., *Mater. Sci. Forum*, 1998, **93**, 278–281.
6. Weckhuysen, B. M. and Schoonheydt, R. A., *Catal. Today*, 1999, **49**, 441–451.
7. Lever, A. B. P., *Inorganic Electronic Spectroscopy (2nd ed.)*. Elsevier, Amsterdam, 1987, p. 507.
8. Brunold, T. C., Güdel, H. U. and Cavalli, E., *Chem. Phys. Lett.*, 1997, **268**, 413–420.
9. O'Neill, H. S t. C. and Navrotski, A., *Am. Miner.*, 1984, **69**, 733–753.
10. Lavrentiev, M. Y u., Purton, J. A. and Allan, N. L., *Am. Miner.*, 2003, **88**, 1522–1531.
11. O'Neill, H. S t. C., Dollase, W. A. and Ross, C. R., *Phys. Chem. Miner.*, 1991, **18**, 302–319.
12. Roelofsen, J. N., Peterson, R. C. and Ramdsepp, M., *Am. Miner.*, 1992, **77**, 522–528.
13. Becker, K. D., *Solid State Ionics*, 2001, **141/142**, 21–30.
14. Lumpkin, G. R., *Prog. Nucl. Energy*, 2001, **38**, 447–454.
15. Weakliem, H. A., *J. Chem. Phys*, 1962, **36**, 2117–2140.
16. Rossano, S., Galoisy, L. and Gwamnesia, G., *Eur. J. Miner.*, 1996, **8**, 471–475.
17. Volkov, V. V., Wang, Z. L. and Zou, B. S., *Chem. Phys. Lett.*, 2001, **337**, 117–124.
18. Galoisy, L. and Calas, G., *Am. Miner.*, 1992, **77**, 677–680.